Area Coverage Using Multiple Aerial Robots with Coverage Redundancy and Collision Avoidance

Soobum Kim, *Graduate Student Member, IEEE*, Ruoyu Lin, *Graduate Student Member, IEEE*, Samuel Coogan, *Senior Member, IEEE*, and Magnus Egerstedt, *Fellow, IEEE*

***Abstract*— This paper presents a coverage control strategy for a team of aerial robots equipped with downward facing cameras. Based on the observation that the resolution of a camera mounted on an aerial robot degrades with the altitude of the robot, we propose a decentralized gradient-based controller that allows each robot to trade off between the size of the area it monitors and the quality of sensing it performs over the area. Moreover, the proposed controller drives a team of robots to a configuration that maximizes the joint probability for detecting targets or events of interest in the coverage domain. To ensure inter-robot collision avoidance during deployment, we utilize control barrier functions to prevent the robots from getting closer to each other than a specified safety distance. The proposed controller is experimentally validated in simulations.**

***Index Terms*— networked control systems, decentralized control, sensor networks**

I. Introduction

THE problem of multi-robot coverage control deals with the distribution of a team of robots over a domain of interest to effectively cover the region to detect signals, events, phenomena, etc [1]. A common formulation of this problem is introduced in [2] where the problem is cast as a locational optimization problem. In such formulation, each robot is responsible for covering an exclusive portion of the domain defined as the Voronoi cell [3] of the robot, and the optimal coverage is obtained when every robot is located at the center of mass of its Voronoi cell, resulting in a centroidal Voronoi tessellation [4] configuration. Variations on the coverage problem have been extensively studied using weighted Voronoi diagrams, e.g., [5], [6], [7]. However, the standard coverage control framework assumes that planar robots cover a planar domain with each robot responsible for a mutually exclusive portion of the domain, which does not hold in the problem concerned in this paper.

The work by S. Kim and S. Coogan was supported by Ford Motor Company and National Science Foundation under Grant No. 1924978. The work by R. Lin and M. Egerstedt was supported by Grant No. CNS-2233783 from the US National Science Foundation.

S. Kim, and S. Coogan are with the School of Electrical and Computer Engineering, Georgia Institute of Technology, Atlanta, GA, USA {skim743, sam.coogan}@gatech.edu

R. Lin and M. Egerstedt are with the Department of Electrical Engineering and Computer Science, University of California, Irvine, CA 92697, USA. Email: {rlin10, magnus}@uci.edu

In this work, we consider a coverage problem where a team of aerial robots equipped with downward facing cameras need to achieve an effective visual coverage over a planar domain of interest. In such scenario, the standard coverage control framework cannot be directly applied as an additional factor, the altitude of each robot, needs to be considered since it directly affects both the robot's quality of sensing and the size of its sensing region. This tradeoff between quality and range is not only present in camera-based systems. It is also of relevance to communication systems, where the quality of the signal deteriorates as a function of the distance, yet is able to cover a broader area as a function of distance, or in acoustic localization systems, where the same quality-range trade-offs appear. In [8], this problem is interpreted as minimizing the size of the area monitored by the number of pixels in the image sensors of robots, i.e., area/pixel, hence maximizing the amount of details acquired from a given area. This formulation was adopted in [9] to visually track wildfire using a team of aerial robots. In [10], [11], a more abstract sensing quality function is used to keep every robot within a specified range of altitudes. Also, each robot's sensing region is defined as the set of points within its field of view where the sensing quality of the robot is better than that of others. In addition to downward facing cameras mounted on robots, cameras with pan/tilt/zoom capabilities are considered in stationary [12] and dynamic [13] settings.

The aforementioned works are similar in the sense that overlapping of sensing regions of robots are discouraged. This is based on the idea that monitoring the same area using multiple cameras does not improve the coverage performance over the area. However, the quality of the image provided by a robot significantly depends on environmental factors such as ambient light conditions or weather conditions at the position of the robot. Accordingly, even if multiple robots are monitoring the same part of an area at the same altitude but at different planar positions, their sensing quality over the area may not be identical. Furthermore, other factors including software or hardware failures of robots can compromise the sensing performance of the robot. Still, such factors are difficult to generalize.

These observations necessitate a coverage control strategy that allows multiple robots to form overlapping sensing regions to account for the uncertainties on their coverage quality, especially for the areas with higher importance. In [14], [15], overlapping of sensing regions of robots are utilized to some

extent to prevent the creation of coverage holes which are unmonitored areas in between the field of views (FOVs) of robots. In contrast to these works, the key idea of this paper is encouraging a team of aerial robots to form overlaps in their sensing regions and using the resulting coverage redundancy to robustly monitor a given area based on the joint probability of detection.

The organization of the paper is as follows. In Section II the sensing model of a robot is defined, and the area coverage problem is formulated as an optimization problem based on the joint probability of detection. In Section III, a decentralized gradient based controller for maximizing the resulting coverage optimization function is derived. The control barrier functions for preventing inter-robot collisions during the deployment are discussed in Section IV. The proposed control strategy is validated in simulations in Section V, and Section VI concludes the paper.

II. Problem Formulation

Consider a coverage control problem, where a planar target domain $\mathcal{D} \subset \mathbb{R}^2$ is to be effectively covered with a team of N aerial robots as described in Fig. 1. Denote the set of robots' indices as $\mathcal{N} = \{1, 2, \dots, N\}$. Each Robot $i \in \mathcal{N}$ has its altitude, $z_i \in \mathbb{R}_{\geq 0}$, as its state in addition to its planar position, $p_i \in \mathbb{R}^2$. In other words, the state vector for Robot i is defined as $x_i = [p_i^\top, z_i]^\top$, and the state vector for the team of robots is denoted as $x = [x_1^\top, x_2^\top, \dots, x_N^\top]^\top$. In this work, each robot is modeled using single integrator dynamics, $\dot{x}_i = u_i$, and we denote $u = [u_1^\top, u_2^\top, \dots, u_N^\top]^\top$. The sensing region of Robot i is assumed to be a disk centered at p_i with radius $r_{s,i}$ where the subscript s denotes 'sensing.' Given the circular field of view (FOV) model described in Fig. 1 where the half-angle field of view of a robot is represented as $0 < \theta < \frac{\pi}{2}$, the sensing radius $r_{s,i}$ can be written as a function of the robot's altitude as $r_{s,i}(z_i) = z_i \tan(\theta)$. Accordingly, the sensing disk can be represented as $B_i(x_i) = \{q \in \mathcal{D} \mid \|p_i - q\| \leq r_{s,i}(z_i)\}$. In general, the performance of a sensor degrades as the distance between the sensor and a signal source increases. Therefore, the quality of coverage provided by a robot for an arbitrary point q can be defined as

$$f(x_i, q) = \begin{cases} g(z_i), & \text{for } q \in B_i(x_i) \\ 0, & \text{otherwise} \end{cases}$$

where $g : \mathbb{R}_{\geq 0} \to \mathbb{R}_{\geq 0}$ is a continuously differentiable strictly decreasing function of z_i. Note that this sensing quality function quantifies the quality of coverage, i.e., image resolution, provided by Robot i for covering a point q, and a higher $f(x_i, q)$ indicates a better sensing quality.

Now, let us define the probability that a robot will actually detect events of interest given its current sensing quality function, $f(x_i, q)$. In general, higher sensing quality yields better detection probability as higher sensing quality implies richer information received by a sensor. Therefore, the probability of detection function of Robot i, P_i, is defined as a continuously differentiable strictly increasing function of its sensing quality function, i.e., $P_i : f \to [0, 1]$ where $\frac{\partial P_i}{\partial f} > 0$. Given the individual probability of detection function, $P_i(f(x_i, q))$, the joint probability of detecting an event at an arbitrary point $q \in \mathcal{D}$ is expressed as the probability of the event not detected by any of the robots covering the point subtracted from the probability of 1. In other words, the joint probability of detection is given as

$$P_{\mathcal{N}_q}(x, q) = 1 - \prod_{k \in \mathcal{N}_q} (1 - P_k(g(z_k)))$$

where $q \in \mathcal{D}$ is an arbitrary point, and $\mathcal{N}_q = \{k \in \mathcal{N} \mid q \in B_k(x_k)\}$ is the set of indices of the robots that are covering point q. Note that $P_{\mathcal{N}_q}(x, q)$ is equivalent to the joint probability of detection evaluated using all robots in the system since $P_k(f(x_k, q)) = 0$ when $q \notin B_k(x_k)$.

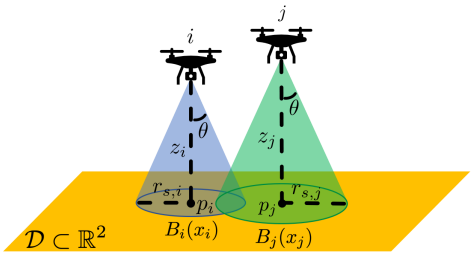

Fig. 1. Two robots at different altitudes with an overlapping sensing region.

Using the definitions of the sensing region of a robot and the joint probability of detection function, we can formulate the following coverage performance function,

$$\mathcal{H}(x) = \int_{B(x)} P_{\mathcal{N}_q}(x, q)\phi(q)dq, \tag{1}$$

which needs to be maximized with respect to the states of the robots, x, to obtain an optimal coverage over a domain. Here, $B(x) = \bigcup_{i=1}^{N} B_i(x_i)$ is the union of the sensing disks of the robots, and $\phi(q) : \mathcal{D} \to \mathbb{R}_{\geq 0}$ is a density function that describes the importance of point q.

Since the sensing quality function of a robot, $g(z_i)$, is a strictly decreasing function of its altitude, a lower altitude yields a higher individual probability of detection, $P_i(g(z_i))$, and a higher joint probability for detecting an event at point q, $P_{\mathcal{N}_q}(x, q)$. However, this makes its sensing disk smaller, which may actually result in a lower coverage performance. Similarly, $P_{\mathcal{N}_q}(x, q)$ increases with the number of robots covering the point, but excessive overlapping may result in a lower coverage performance as the total area of the union of the sensing disks become smaller. Therefore, each robot needs to balance between how much area it covers and how well it covers the area. At the same time, each robot needs to optimize the amount of overlapping of its sensing disk with other robots' sensing disks in a way that maximizes the joint probability of detection.

In general, the dynamics of aerial vehicles change during take off due to factors such as ground effect. Therefore, we make the following assumption throughout the paper.

Assumption 1. *All robots are initialized to non-zero altitudes before being deployed for the coverage.*

Note that the value of the coverage performance function $\mathcal{H}(x)$ is lower bounded by 0, which is achieved when $z_i = 0$

for all robots in the team. Since $\mathcal{H}(x)$ needs to be maximized for an optimal coverage, Assumption 1 does not constrain the optimization problem.

III. Gradient Ascent Controller

In this section, a decentralized controller that maximizes the coverage performance function (1) is derived. The coverage performance function is in general non-convex, and one way to maximize the function is to use a gradient ascent controller to obtain a local maximum of the function. We state the form of the gradient of the coverage performance function (1) as a theorem as follows.

Theorem 1. *The gradient of the coverage performance function* (1) *with respect to the position of Robot i, x_i, is given as*

$$\frac{\partial \mathcal{H}(x)}{\partial x_i} = \begin{bmatrix} \frac{1}{z_i \tan(\theta)} m^p_{b,i}(x) \left(c^p_{b,i}(x) - p_i \right) \\ \frac{\partial P_i(g(z_i))}{\partial z_i} m^p_i(x) + \tan(\theta) m^p_{b,i}(x) \end{bmatrix}^\top$$

where

$$m^p_i(x) = \int_{B_i(x_i)} \left(1 - P_{\mathcal{N}_q \setminus \{i\}}(x,q)\right) \phi(q) dq,$$

$$m^p_{b,i}(x) = \int_{\partial B_i(x_i)} \left(P_{\mathcal{N}_q}(x,q) - P_{\mathcal{N}_q \setminus \{i\}}(x,q)\right) \phi(q) dq,$$

$$c^p_{b,i}(x) = \frac{\int_{\partial B_i(x_i)} q \left(P_{\mathcal{N}_q}(x,q) - P_{\mathcal{N}_q \setminus \{i\}}(x,q)\right) \phi(q) dq}{m^p_{b,i}(x)}$$

are the probability weighted mass, boundary mass, and the center of mass of the boundary of the sensing disk of the robot, $B_i(x_i)$, respectively.

Proof. In order to facilitate the gradient analysis, the coverage performance function is first rewritten as

$$\begin{aligned} \mathcal{H}(x) = &\int_{B_i(x_i)} P_{\mathcal{N}_q}(x,q) \phi(q) dq \\ &+ \int_{B(x) \setminus B_i(x_i)} P_{\mathcal{N}_q \setminus \{i\}}(x,q) \phi(q) dq \end{aligned} \tag{2}$$

where the first term is the coverage performance function evaluated over the sensing disk of an arbitrary Robot i, and the second term is the coverage performance evaluated over the rest of the union of the sensing disks. Here, $\setminus$ denotes the set difference operator.

The gradient of the coverage performance function (2) can be expressed as $\frac{\partial \mathcal{H}(x)}{x_i} = [\frac{\partial \mathcal{H}(x)}{\partial p_i}, \frac{\partial \mathcal{H}(x)}{\partial z_i}]$. For clarity, the gradient of the function with respect to the altitude of Robot i is derived first. Following Leibniz integral rule [4], one can obtain the gradient as

$$\begin{aligned} \frac{\partial \mathcal{H}(x)}{\partial z_i} = &\int_{B_i(x_i)} \frac{\partial}{\partial z_i} P_{\mathcal{N}_q}(x,q) \phi(q) dq \\ &+ \int_{\partial B_i(x_i)} P_{\mathcal{N}_q}(x,q) \vec{n}_i^\top(q) \frac{\partial q}{\partial z_i} \phi(q) dq \\ &+ \int_{\partial (B(x) \setminus B_i(x_i))} P_{\mathcal{N}_q \setminus \{i\}}(x,q) \vec{n}^\top_{B \setminus B_i}(q) \frac{\partial q}{\partial z_i} \phi(q) dq \end{aligned} \tag{3}$$

where the first two integral terms are computed from the first term in (2), and the last boundary integral term is obtained from the second term in (2). The terms $\vec{n}_i(q)$ and $\vec{n}_{B \setminus B_i}(q)$ are the unit outward normal vectors of $B_i(x_i)$ and $B(x) \setminus B_i(x)$, respectively.

In order to efficiently compute the gradient, the boundary integral terms need to be simplified. Note that the second boundary integral term is non-zero only for the points $q \in \partial(B(x) \setminus B_i(x_i)) \cap \partial B_i(x_i)$ due to the term, $\frac{\partial q}{\partial z_i}$, in the integrand. Accordingly, thanks to the $P_{\mathcal{N}_q \setminus \{i\}}(x,q)$ term, we can let $\partial \left(B(x) \setminus B_i(x_i)\right) = \partial B_i(x_i)$ and $\vec{n}_{B \setminus B_i}(q) = -\vec{n}_i(q)$. The unit outward normal vector $\vec{n}_i(q)$ can be easily computed as $B_i(x_i)$ is a circle centered at p_i, i.e., $B_i(x_i) = \{q \in \mathcal{D} \mid \|p_i - q\| \leq r_{\mathrm{s},i}(z_i)\}$. In fact, $B_i(x_i)$ is a circular region inside the coverage domain $\mathcal{D}$, and $\partial B_i(x_i)$ may contain points in $\partial \mathcal{D}$ which are not necessarily circular arcs. However, the points on the boundary of the domain $\mathcal{D}$ do not depend on the states of robots, and these points do not affect the value of the boundary integrals as $\frac{\partial q}{\partial z_i} = 0, \ \forall q \in \partial \mathcal{D}$. Therefore, for brevity, we simply denote $\partial B_i(x_i) \setminus \partial \mathcal{D}$ as $\partial B_i(x_i)$ in the rest of the paper. For any point $q \in \partial B_i(x_i)$, it holds that $\|p_i - q\| = r_{\mathrm{s},i}(z_i)$. Differentiating both sides of the equation with respect to z_i yields

$$\frac{(q - p_i)^\top}{\|p_i - q\|} \frac{\partial q}{\partial z_i} = \tan(\theta). \tag{4}$$

Note that $r_{\mathrm{s},i}(z_i) = z_i \tan(\theta)$, and $\frac{(q-p_i)^\top}{\|p_i - q\|} = \vec{n}_i^\top(q)$. According to Assumption 1, we do not consider the singularity case on the left hand side of (4) obtained when $p_i = \partial B_i(x_i) = q$, which occurs if and only if $z_i = 0$.

With the above results, the gradient expression in (3) can be simplified to

$$\begin{aligned} \frac{\partial \mathcal{H}(x)}{\partial z_i} = &\frac{\partial P_i(g(z_i))}{\partial z_i} \int_{B_i(x_i)} \left(1 - P_{\mathcal{N}_q \setminus \{i\}}(x,q)\right) \phi(q) dq \\ &+ \tan(\theta) \int_{\partial B_i(x_i)} \left(P_{\mathcal{N}_q}(x,q) - P_{\mathcal{N}_q \setminus \{i\}}(x,q)\right) \phi(q) dq. \end{aligned} \tag{5}$$

Since the sensing quality function $g(z_i)$ is a strictly decreasing function of z_i, and the individual probability of detection function $P_i(g(z_i))$ is a strictly increasing function of $g(z_i)$, $P_i(g(z_i))$ is a strictly decreasing function of z_i, i.e., $\frac{\partial P_i(g(z_i))}{\partial z_i} < 0$. Accordingly, the first term of (5) is negative, and the term is the component of the gradient that tries to bring Robot i down to the ground. On the other hand, the second term of the gradient is positive since $P_{\mathcal{N}_q}(x,q) > P_{\mathcal{N}_q \setminus \{i\}}(x,q), \ \forall q \in \partial B_i(x_i)$. Therefore, it is the component of the gradient that tries to lift the altitude of the robot.

The gradient of the coverage performance function (2) with respect to the planar position of Robot i can be derived using a similar analysis. Utilizing Leibniz integral rule [4] yields the gradient expression as

$$\begin{aligned} \frac{\partial \mathcal{H}(x)}{\partial p_i} = &\int_{\partial B_i(x_i)} P_{\mathcal{N}_q}(x,q) \vec{n}_i^\top(q) \frac{\partial q}{\partial p_i} \phi(q) dq \\ &+ \int_{\partial (B(x) \setminus B_i(x_i))} P_{\mathcal{N}_q \setminus \{i\}}(x,q) \vec{n}^\top_{B \setminus B_i}(q) \frac{\partial q}{\partial p_i} \phi(q) dq. \end{aligned} \tag{6}$$

Note that (6) only has boundary integral terms since $\frac{\partial}{\partial p_i} P_{\mathcal{N}_q}(x,q) = 0,\ \forall q \in B_i(x_i)$. As in the gradient analysis for the vertical component, we can let $\partial\left(B(x) \setminus B_i(x_i)\right) = \partial B_i(x_i)$ and $\vec{n}_{B\setminus B_i}(q) = -\vec{n}_i(q)$. The expression $\vec{n}_i(q)\frac{\partial q}{\partial p_i}$ can be simplified using the relationship, $\|p_i - q\| = r_{\mathrm{s},i}(z_i),\ \forall q \in \partial B_i(x_i)$. Differentiating both sides of the equation with respect to p_i and reorganizing terms yield

$$\frac{(q-p_i)^\top}{\|p_i - q\|}\frac{\partial q}{\partial p_i} = \frac{(q-p_i)^\top}{z_i \tan(\theta)} \tag{7}$$

where the left hand side of (7) is $\vec{n}_i(q)\frac{\partial q}{\partial p_i}$. Note that $\|p_i - q\| = z_i \tan(\theta),\ \forall q \in \partial B_i(x_i)$. Rewriting the planar component of the gradient using the above results gives

$$\begin{aligned}\frac{\partial \mathcal{H}(x)}{\partial p_i} = \frac{1}{z_i \tan(\theta)} \int_{\partial B_i(x_i)} \big(P_{\mathcal{N}_q}(x,q) \\ - P_{\mathcal{N}_q \setminus \{i\}}(x,q)\big)(q-p_i)^\top \phi(q) dq.\end{aligned} \tag{8}$$

Substituting the definitions of $m_i^p(x), m_{b,i}^p(x)$ and, $c_{b,i}^p(x)$ into (5) and (8) concludes the proof. □

Note that the gradient depends on the probability weighted mass $m_i^p(x)$ and the probability weighted boundary mass $m_{b,i}^p(x)$ of the sensing disk of the robot. Since this can make the magnitude of the gradient negligibly small if a robot is covering a low density region, we multiply the gradient by a positive and state dependent gain, $\gamma_i(x) = \frac{K}{m_i^p(x)} > 0$, to obtain a gradient ascent controller,

$$\begin{aligned} u_i = \begin{bmatrix} u_{p,i} \\ u_{z,i} \end{bmatrix} &= \gamma_i(x) \frac{\partial \mathcal{H}(x)}{\partial x_i}^\top \\ &= K \begin{bmatrix} \frac{1}{z_i \tan(\theta)} \frac{m_{b,i}^p(x)}{m_i^p(x)} (c_{b,i}^p(x) - p_i) \\ \frac{\partial P_i(g(z_i))}{\partial z_i} + \tan(\theta) \frac{m_{b,i}^p(x)}{m_i^p(x)} \end{bmatrix}. \end{aligned} \tag{9}$$

This way, the magnitude of the gradient depends on the ratio between $m_i(x_i)$ and $m_{b,i}(x_i)$ rather than their actual values.

Remark 1. *Although the compact notation of* (9) *suggests that each robot's control input relies on the states of all robots, x, we note that only the states of neighboring robots with overlapping sensing regions are actually needed.*

With the gradient ascent controller, we obtain the following proposition.

Proposition 1. *The coverage performance function* (1) *for a team of robots driven by the gradient ascent controller in* (9) *is always non-decreasing, and all robots asymptotically converge to stationary positions.*

Proof. Since the joint probability of detection at point q inside the coverage domain $\mathcal{D}$ has a value between 0 and 1, i.e., $0 \le P_{\mathcal{N}_q}(x,q) \le 1$, the coverage performance function $H(x)$ is upper-bounded by $\mathcal{H}_{max} = \int_{\mathcal{D}} \phi(q) dq$ where the joint probability of detection is 1 across the whole domain. Now, we can define a dual of the coverage performance function as $\tilde{\mathcal{H}}(x) = \mathcal{H}_{max} - \mathcal{H}(x)$. Assuming single integrator dynamics, $\dot{x}_i = u_i$, the time derivative of the dual function is given as

$$\begin{aligned}\dot{\tilde{\mathcal{H}}}(x) &= -\sum_{i=1}^{N} \frac{\partial \mathcal{H}(x)}{\partial x_i}\dot{x}_i = -\sum_{i=1}^{N} \frac{\partial \mathcal{H}(x)}{\partial x_i}\Gamma_i(x)\frac{\partial \mathcal{H}(x)}{\partial x_i}^\top \\ &\le 0\end{aligned} \tag{10}$$

where $\Gamma_i(x) = \gamma_i(x) I_{3\times 3}$ is a diagonal matrix with $I_{3\times 3}$ being a 3 by 3 identity matrix. The time derivative $\dot{\tilde{\mathcal{H}}}(x)$ is always non-positive since $\Gamma_i(x_i)$ is positive definite for all Robot i. Now, let us define a set, $\mathcal{S} = \left\{x \mid \dot{\tilde{\mathcal{H}}}(x) = \dot{\mathcal{H}}(x) = 0\right\}$, and the largest invariant set of $\mathcal{S}$ as $\mathcal{M}$. According to (10), $\dot{\tilde{\mathcal{H}}}(x) = 0$ if and only if $u_i = \frac{\partial \mathcal{H}(x)}{\partial x_i}^\top = 0$ for all Robot i. Therefore, $\mathcal{S} = \mathcal{M} = \{x \mid u = 0\}$, and by LaSalle's invariance principle, it holds that $x \to \mathcal{M}$ as $t \to \infty$. □

From (9), we know that the optimal planar position of a robot is given as $c_{b,i}^p(x_i)$. On the other hand, the behavior of the vertical component of the gradient is unclear as its equilibrium condition is not given in a closed-form. In order to provide further analysis, we use the sensing quality function of $g(z_i) = \frac{1}{z_i^2}$ based on the observation that the area of the sensing disk of a robot is proportional to the robot's altitude squared. Also, we let the individual probability of detection function $P_i(g(z_i)) = \frac{g(z_i)}{g(z_i)+1}$ to map the sensing quality to $[0,1]$, which yields $P_i(g(z_i)) = \frac{1}{z_i^2+1}$. With the sensing quality and individual probability of detection functions, the gradient ascent controller for the altitude simplifies to

$$u_{z,i} = -\frac{2z_i}{(z_i^2+1)^2} + \tan(\theta)\frac{m_{b,i}^p(x)}{m_i^p(x)}. \tag{11}$$

As discussed previously, this vertical component of the controller allows a robot to balance between how much area it covers and how well it covers the area.

Remark 2. *Although the gradient analysis in* (11) *is performed using specific g and P_i, similar results to* (11) *hold for different functions as long as $g : \mathbb{R}_{\ge 0} \to \mathbb{R}_{\ge 0}$ is a strictly decreasing function, and $P_k : g \to [0,1]$ is a strictly increasing function.*

In case of deploying single robot, i.e., $N = 1$, with a uniform density function of $\phi(q) = 1$ applied to the domain, $P_{\mathcal{N}_q}(x,q)$ reduces to $P_i(g(z_i)) = \frac{1}{z_i^2+1}$. Accordingly, $m_i^p(x) = \pi r_{\mathrm{s},i}^2(z_i)$ and $m_{b,i}^p(x) = \frac{2\pi r_{\mathrm{s},i}(z_i)}{z_i^2+1}$. Since $r_{\mathrm{s},i}(z_i) = z_i \tan(\theta)$, the controller (11) simplifies to

$$u_{z,i} = \frac{1}{z_i(z_i^2+1)^2},$$

which implies that the robot will keep increasing its altitude with a decreasing rate, i.e., $u_{z,i} \to 0$ as $z_i \to \infty$.

Remark 3. *In reality, the robot converges to an equilibrium altitude since the coverage domain $\mathcal{D} \subset \mathbb{R}^2$ is finite. As the altitude of the robot becomes high enough, parts of its circular boundary, $\partial B_i(x_i)$, start to lie outside of $\mathcal{D}$, and this results in a smaller $m_{b,i}^p(x)$ hence decreased control input.*

IV. Control Barrier Functions for Collision Avoidance

The successful deployment of multiple aerial robots is often premised on inter-robot collision avoidance. To prevent collisions between robots, the distance between any pair of robots needs to be greater than a safety distance at all times. However, it is difficult to derive the minimum possible distance between any pair of robots that can be obtained with the gradient ascent controller (9) as it largely depends on the density function applied to the domain. To address this issue, we utilize control barrier functions (CBFs) [16].

Given single integrator robot dynamics, $\dot{x}_i = u_i$, we can define the safe set of states of an agent as $\mathcal{C} = \{x_i \in \mathcal{D} \mid h(x_i) \geq 0\}$ where $h(x_i)$ is a continuously differentiable function. The function $h(x_i)$ is a control barrier function if there exists a class $\mathcal{K}$ function α such that

$$\sup_{u_i \in \mathcal{U}_i} \left\{ \frac{d}{dt} h(x_i) \right\} \geq -\alpha(h(x_i))$$

for all $x_i \in \mathcal{D}$. Here, $\mathcal{U}_i$ is the set of admissible inputs.

To prevent the robots from colliding with each other, we enforce the inter-robot distance constraint $\|x_i - x_j\| \geq d_{\text{safe}}, \forall i, j \in \mathcal{N},\ i \neq j$ where $d_{\text{safe}} > 0$ is the minimum safety distance between a pair of robots. Therefore, we can define the collision avoidance CBF, $h_{ij}(x_i, x_j) = \|x_i - x_j\|^2 - d_{\text{safe}}^2 \geq 0$, whose time derivative is given as

$$\frac{d}{dt} h_{ij}(x_i, x_j) = 2(x_i - x_j)^\top u_i - 2(x_i - x_j)^\top u_j.$$

Accordingly, similar to what was done in [17], the quadratic programming (QP) controller that composites the closest control input to the gradient ascent controller in (9) in the sense of l_2 norm while satisfying the minimum distance constraint between every robot can be formulated as

$$\begin{aligned} u^* = \arg\min_{u} & \sum_{i=1}^{N} \|u_i - \hat{u}_i\|^2 \\ \text{s.t. } & 2(x_i - x_j)^\top (u_i - u_j) \geq -\alpha(h_{ij}(x_i, x_j)),\ \forall j \neq i \end{aligned} \tag{12}$$

where $\hat{u}_i$ is the nominal control input for Robot i given by (9), and α is a class $\mathcal{K}$ function.

Although the QP controller in (12) prevents potential inter-robot collisions, it is a centralized approach as it requires the nominal control input for each robot, $\hat{u}_i$, and the positions of all robots, x. Since the nominal controller of a robot in (9) is decentralized in the sense that it only requires the position of the robot itself and the positions of its neighboring robots that have overlapping sensing regions with the robot, a decentralized version of the QP controller is needed to keep the controller for each robot decentralized. According to [18], a decentralized implementation of the QP controller in (12) for collision avoidance is given as

$$\begin{aligned} u_i^* = \arg\min_{u_i} & \|u_i - \hat{u}_i\|^2 \\ \text{s.t. } & 2(x_i - x_j)^\top u_i \geq -\frac{\alpha(h_{ij}(x_i, x_j))}{2},\ \forall j \in \mathcal{N}_i \end{aligned} \tag{13}$$

where $\mathcal{N}_i = \{j \in \mathcal{N} \mid \|p_i - p_j\| \leq r_{\text{s},i}(z_i) + r_{\text{s},j}(z_j), i \neq j\}$ is the set of neighbors of Robot i whose sensing disks overlap with that of Robot i. The derivation of (13) is based on the fact that (12) is a convex optimization problem, which allows for the independent computation of each u_i by ensuring that every robot satisfies the half of each pair-wise barrier constraints. Due to space constraints, we refer the reader to [18] and references therein for a thorough discussion. This decentralized QP controller (13) requires the same information needed to compute the nominal gradient ascent controller in (9), which effectively keeps the controller for each robot to be decentralized.

V. Experimental Results

In this section, the effectiveness of the nominal controller (9) and the QP controller with collision avoidance (13) are experimentally validated in simulations. For the experiments, a rectangular domain $\mathcal{D}$ is used where the dimensions are $[-1.6, 1.6]$ for the X axis and $[-1.0, 1.0]$ for the Y axis with $[0, 0]$ being the origin. For the density function, a bimodal Gaussian distribution function,

$$\phi(q) = \frac{1}{4\pi\sqrt{|\Sigma|}} \sum_{i=1}^{2} \exp\left(-\frac{1}{2}(q - \mu_i)^\top \Sigma^{-1} (q - \mu_i) \right),$$

is used where μ_i is the mean of the i^{th} mode, and Σ is the covariance matrix.

A total of 5 robots were deployed for the experiment where the density function parameters are set to $\mu_1 = [1.0, 0.0]^\top, \mu_2 = [-1.0, 0.0]^\top$, and $\Sigma = 0.3 I_{2\times 2}$. The initial positions, final positions without CBFs, and final positions with CBFs are shown in Fig. 2. For the initial condition illustrated in Fig. 2a, two robots end up covering the left mode of the density, and other three robots converge to positions close to the right mode of the density. Since the coverage performance function (1) to be optimized is in general non-convex, and the controller in (9) is a gradient-based controller, it is worth noting that the number of robots converging to each mode of the density varies with the initial positions of the robots.

In this experiment, Robot 3 was initialized at a higher altitude than that of other robots to demonstrate that the proposed controller allows the sensing disk of a robot to be completely contained within the sensing disk of another robot. From Fig. 2b and Fig. 2c, it can be observed that the gradient ascent controller (9) without CBFs drives each robot to unique position, and the QP controller (13) allows the robots to converge to final positions similar to those obtained in Fig. 2b but maintain a farther minimum inter-robot distance. In both cases, the robots converge to a configuration where they effectively form coverage redundancy around high density regions. The evolution of the coverage performance function (1) during the deployment is shown in Fig. 3a. As predicted in Proposition 1, the coverage performance is always non-decreasing and converge to a local optimum for the case without CBFs. Similar result is obtained with CBFs with slight decrease in the coverage performance. In addition to the coverage performance plot, the minimum barrier value of each robot, i.e., $h_i^{\min} = \min_j h_{ij}(x_i, x_j)$ is shown in Fig. 3b. Every minimum barrier value remains greater than 0, implying that

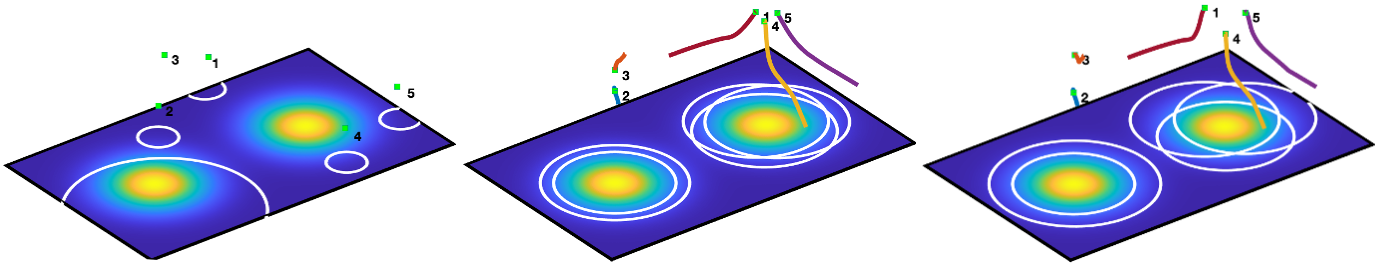

(a) Initial Configuration (b) Final Configuration without CBFs (c) Final Configuration with CBFs

Fig. 2. The (a) initial configuration, (b) final configuration without CBFs, and (c) final configuration with CBFs of 5 robots. The color gradation in the background visualizes the applied density function where colors close to yellow indicate higher density. Each white circle is the sensing disk of a robot, and the trajectories of the robots are shown as colored lines.

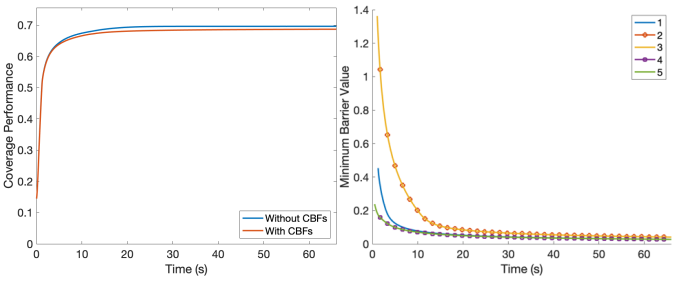

(a) Coverage Performance (b) Minimum Barrier Value

Fig. 3. The evolution of the coverage performance (a) and the minimum barrier values (b) during the experiment.

all robots indeed maintained a safety distance from each other. In fact, although the CBF-based formulation provides safety guarantees as well as supports decentralized formulations, it is not necessarily optimal from a performance vantage-point as the use of CBFs no longer guarantees the monotonic increase of the coverage performance function. Additional work is needed to fully elucidate this issue and is left as a future endeavor.

VI. CONCLUSIONS

In this paper, we proposed a decentralized coverage controller for a team of aerial robots equipped with downward facing cameras to effectively cover a given domain utilizing coverage redundancy. The coverage performance function for a multi-robot team was formulated based on the joint probability of detection provided by the robots covering common areas, and a gradient ascent controller that maximizes this performance measure was derived. To ensure inter-robot collision avoidance, control barrier functions were utilized. The proposed controller is decentralized in the sense that each robot only requires the positions of the robots whose sensing disks overlap with its own. Both the nominal controller and the controller with the decentralized CBFs were validated using simulations involving 5 robots.

REFERENCES

[1] J. Cortes and M. Egerstedt, "Coordinated control of multi-robot systems: A survey," *SICE Journal of Control, Measurement, and System Integration*, vol. 10, no. 6, pp. 495–503, 2017.

[2] J. Cortes, S. Martinez, T. Karatas, and F. Bullo, "Coverage control for mobile sensing networks," *IEEE Transactions on Robotics and Automation*, vol. 20, no. 2, pp. 243–255, 2004.

[3] A. Okabe, B. Boots, K. Sugihara, and S. N. Chiu, *Spatial Tessellations: Concepts and Applications of Voronoi Diagrams*. New York, NY, USA: John Wiley & Sons, Inc., 2000.

[4] Q. Du, V. Faber, and M. Gunzburger, "Centroidal voronoi tessellations: Applications and algorithms," *SIAM Review*, vol. 41, no. 4, pp. 637–676, 1999.

[5] L. C. A. Pimenta, V. Kumar, R. C. Mesquita, and G. A. S. Pereira, "Sensing and coverage for a network of heterogeneous robots," in *2008 47th IEEE Conference on Decision and Control*, 2008, pp. 3947–3952.

[6] A. Pierson, L. C. Figueiredo, L. C. Pimenta, and M. Schwager, "Adapting to sensing and actuation variations in multi-robot coverage," *The International Journal of Robotics Research*, vol. 36, no. 3, pp. 337–354, 2017.

[7] S. Kim, M. Santos, L. Guerrero-Bonilla, A. Yezzi, and M. Egerstedt, "Coverage control of mobile robots with different maximum speeds for time-sensitive applications," *IEEE Robotics and Automation Letters*, vol. 7, no. 2, pp. 3001–3007, 2022.

[8] M. Schwager, B. J. Julian, M. Angermann, and D. Rus, "Eyes in the sky: Decentralized control for the deployment of robotic camera networks," *Proceedings of the IEEE*, vol. 99, no. 9, pp. 1541–1561, 2011.

[9] H. X. Pham, H. M. La, D. Feil-Seifer, and M. Deans, "A distributed control framework for a team of unmanned aerial vehicles for dynamic wildfire tracking," in *2017 IEEE/RSJ International Conference on Intelligent Robots and Systems (IROS)*, 2017, pp. 6648–6653.

[10] S. Papatheodorou, A. Tzes, and Y. Stergiopoulos, "Collaborative visual area coverage," *Robotics and Autonomous Systems*, vol. 92, pp. 126–138, 2017.

[11] Y. Wang, J. Fu, M. Tang, S. Wang, and G. Wen, "Collision avoidance visual coverage control of multiple second-order mobile aerial agents," in *2023 International Conference on Advanced Robotics and Mechatronics (ICARM)*, 2023, pp. 439–444.

[12] O. Arslan, H. Min, and D. E. Koditschek, "Voronoi-based coverage control of pan/tilt/zoom camera networks," in *2018 IEEE International Conference on Robotics and Automation (ICRA)*, 2018, pp. 5062–5069.

[13] N. Bousias, S. Papatheodorou, M. Tzes, and A. Tzes, "Collaborative visual area coverage using aerial agents equipped with ptz-cameras under localization uncertainty," in *2019 18th European Control Conference (ECC)*, 2019, pp. 1079–1084.

[14] R. Funada, M. Santos, J. Yamauchi, T. Hatanaka, M. Fujita, and M. Egerstedt, "Visual coverage control for teams of quadcopters via control barrier functions," in *2019 International Conference on Robotics and Automation (ICRA)*, 2019, pp. 3010–3016.

[15] R. Funada, M. Santos, R. Maniwa, J. Yamauchi, M. Fujita, M. Sampei, and M. Egerstedt, "Distributed coverage hole prevention for visual environmental monitoring with quadcopters via nonsmooth control barrier functions," *IEEE Transactions on Robotics*, pp. 1–20, 2023.

[16] A. D. Ames, S. Coogan, M. Egerstedt, G. Notomista, K. Sreenath, and P. Tabuada, "Control barrier functions: Theory and applications," in *2019 18th European Control Conference (ECC)*, 2019, pp. 3420–3431.

[17] A. D. Ames, X. Xu, J. W. Grizzle, and P. Tabuada, "Control barrier function based quadratic programs for safety critical systems," *IEEE Transactions on Automatic Control*, vol. 62, no. 8, pp. 3861–3876, 2017.

[18] L. Wang, A. D. Ames, and M. Egerstedt, "Safety barrier certificates for collisions-free multirobot systems," *IEEE Transactions on Robotics*, vol. 33, no. 3, pp. 661–674, 2017.